

**Spin-Crossover in the Complex  
Bis(*cis*-1,2-dicyano-1,2-ethylenedithiolato)-  
[2-(*p*-pyridyl)-4,4,5,5-tetramethylimidazolinium]-  
iron(III)**

Mohammed Fettouhi,<sup>\*,†</sup> Mohammed Morsy,<sup>†</sup>  
Abdel Waheed,<sup>†</sup> Stéphane Golhen,<sup>‡</sup>  
Lahcène Ouahab,<sup>\*,‡</sup> Jean-Pascal Sutter,<sup>§</sup>  
Olivier Kahn,<sup>§</sup> Nieves Menendez,<sup>||</sup> and  
François Varret<sup>||</sup>

Chemistry Department, King Fahd University of Petroleum  
and Minerals, P.O. Box 5048, Dahrhan 31261, Saudi Arabia,  
Laboratoire de Chimie du Solide et Inorganique Moléculaire,  
UMR 6511, Groupe Matériaux Moléculaires, Université de  
Rennes 1, Campus Beaulieu 35042, Rennes Cedex, France,  
Laboratoire des Sciences Moléculaires, ICMCB,  
UPR CNRS 9048, F-33608 Pessac, France, and Laboratoire  
de Magnétisme et d'Optique, CNRS—Université de  
Versailles (UMR 8634), 78035 Versailles Cedex, France

Received March 16, 1999

**Introduction**

A great deal of interest was devoted in the 1960s and 1970s to the five-coordinate adducts of dithiolene complexes  $[M(S_2C_2R_2)_2L]^{n-}$  obtained by the dissociation of the  $[M(S_2C_2R_2)_2]^{2n-}$  ( $M = Fe, Co$ ) dimers and addition of Lewis bases such as pyridines, phosphines, and stibines. Many of these complexes are labile when dissolved in polar or non polar solvents. They dissociate into the free Lewis base and the precursor, or they exist in equilibrium between the adduct and its components. This lability is particularly marked in most of the pyridine and substituted pyridine complexes.<sup>1–2</sup> The majority of these complexes exhibit multiple electron transfer processes for which the oxidation state of the ligand is still not determined unequivocally. Their ability to activate molecular oxygen was equally reported.<sup>3</sup> ESR investigations showed that molecules in solution are subject to different distortions due to solvent interactions in addition to the reversible formation of six-coordinate  $[Co(S_2C_2R_2)_2L_2]^{n-}$  in the presence of an excess of  $L$ .<sup>4,5</sup> The reactivity of these species in solution is at the origin of the difference of spin values measured in solution and the solid state.<sup>2</sup> Adducts containing weak-field ligands have the intermediate spin ( $S = 3/2$ ) whereas strong-field ligand complexes are low spin ( $S = 1/2$ ). In a recent communication we have reported the occurrence of spin crossover in a five coordinate iron complex with a nitroxide-based molecule as axial ligand accompanied by an intramolecular spin–spin interaction.<sup>6</sup>

**Table 1.** Crystal Parameters and X-ray Diffraction Data

empirical formula	C <sub>26</sub> H <sub>32</sub> FeN <sub>9</sub> O <sub>2</sub> S <sub>4</sub>
fw	686.70
space group	C2/c
<i>a</i> , Å	17.755(16)
<i>b</i> , Å	13.620(4)
<i>c</i> , Å	13.832(17)
$\beta$ , deg	100.04(5)
<i>V</i> , Å <sup>3</sup>	3293(5)
$\rho$ , (calcd) g cm <sup>-3</sup>	1.385
<i>Z</i>	4
$\mu$ , mm <sup>-1</sup>	0.750
wavelength, Å	0.710 73
temperature, K	293(2)
<i>R</i> <sub>1</sub> [ $I \geq 2\sigma(I)$ ] <sup>a</sup>	0.0542
wR <sub>2</sub> [ $I \geq 2\sigma(I)$ ] <sup>b</sup>	0.1030

$$^a R_1 = \sum |F_o| - |F_c| / \sum |F_o|. \quad ^b wR_2 = \{ \sum [w(F_o^2 - F_c^2)^2] / \sum [w(F_o^2)^2] \}^{1/2}.$$

This compound is namely  $Fe(mnt)_2(rad)$  where *mnt* is maleonitrile dithiolato and *rad* is 2-(*p*-pyridyl)-4,4,5,5-tetramethylimidazoline-1-oxyl. We present herein the magnetic and Mössbauer characterizations of a new case of spin crossover in a new zwitterionic bis(maleonitrile dithiolato) five-coordinate complex together with its synthesis and X-ray structure. The compound is bis(*cis*-1,2-dicyano-1,2-ethylenedithiolato)[2-(*p*-pyridyl)-4,4,5,5-tetramethylimidazolinium]iron(III)·2DMF,  $[Fe(mnt)_2(idzm)] \cdot 2DMF$ .

**Experimental Section**

**Synthesis.** 2-(*p*-Pyridyl)-4,4,5,5-tetramethylimidazoline-1-oxyl-3-oxide [NITpPy] and sodium bis(*cis*-1,2-dicyano-1,2-ethylenedithiolato)iron(III)  $[NaFe(mnt)_2]$  were prepared following literature procedures.<sup>7,8</sup> A 0.39 g amount of  $NaFe(mnt)_2$  was dissolved in 60 mL of acetonitrile containing two drops of ethanolic sulfuric acid (20%). 0.3 g NITpPy (0.3 g) was then added as a solid, and the mixture was refluxed for 30 min. The solution turned light brown and a brown precipitate formed. It was recrystallized from dimethylformamide to give solvated brown needle-shaped crystals of formula  $Fe(mnt)_2(idzm) \cdot 2DMF$ . Anal. Obsd (calcd) for  $FeS_4N_9C_{26}H_{32}O_2$ : Fe, 8.56 (8.14); S, 18.70 (18.66); N, 18.51 (18.37); C, 45.57 (45.49); H, 4.80 (4.67). IR (KBr): 2204, 1660, 1590, 1542, 1502, 1432, 1414, 1388, 1252, 1220, 668, 574, 506 cm<sup>-1</sup> UV–vis: cm<sup>-1</sup> ( $\epsilon$  (L/mol cm<sup>-1</sup>)  $\times 10^{-3}$ ): 20 747 (2.3); 23 267 (3.1); 26 969 (7.7); 37 010 (13.4).

**Crystallographic Data Collection and Structure Determination.**

A single crystal was mounted on an Enraf-Nonius CAD4 diffractometer equipped with a graphite monochromated Mo K $\alpha$  radiation source ( $\lambda = 0.710 73$  Å). Cell dimensions and orientation matrix for data collection were obtained from least-squares refinement, using the setting angles of 25 centered reflections. Crystal data are summarized in Table 1. Intensities were collected by  $\theta$ – $2\theta$  scans. No significant decay was revealed on the three standard reflections measured every hour during data collection. Lorentz polarization and semiempirical absorption corrections ( $\psi$ -scan method) were applied to intensities for all data. Scattering factors and corrections for anomalous dispersion were taken from ref 9. Structure was solved with SHELXS-97<sup>10</sup> and refined with SHELXL-97<sup>10</sup> programs by full-matrix least-squares method, on  $F^2$ .

Selected bond distances and bond angles are given in Table 2, and complete crystal structure results are given as Supporting Information.

<sup>†</sup> King Fahd University of Petroleum and Minerals.

<sup>‡</sup> Université de Rennes 1.

<sup>§</sup> ICMCB.

<sup>||</sup> Université de Versailles.

(1) McCleverty, J. A.; Atherton, N. M.; Connelly, N. G.; Winscom, C. J. *J. Chem. Soc. (A)* **1969**, 2242.

(2) Connelly, N. G.; McCleverty, J. A.; Winscom, C. J. *Nature* **1967**, 216, 999.

(3) Epstein, E. F.; Bernal I.; Balch, A. L. *J. Chem. Soc., Chem. Commun.* **1970**, 136.

(4) Carpenter, G. B.; Clark, G. S.; Rieger, A. L.; Rieger, P. H.; Sweigart, D. A. *J. Chem. Soc., Dalton. Trans* **1994**, 2903 and references therein.

(5) Nochomovitz, Y. D.; Rieger, A. L.; Rieger, P. H.; Roper, B. J. *J. Chem. Soc., Dalton. Trans.* **1996**, 3503.

(6) Sutter, J. P.; Fettouhi, M.; Li, L.; Michaut, C.; Ouahab, L.; Kahn, O. *Angew. Chem., Int. Ed. Engl.* **1996**, 35, 2113.

(7) Davison, A.; Holm, R. H. *Inorg. Synth.* **1967**, 10, 1.

(8) Ullman, E. F.; Osiecki, J. H.; Boocock, D. G. B.; Darey, R. *J. Am. Chem. Soc.* **1972**, 94, 7049.

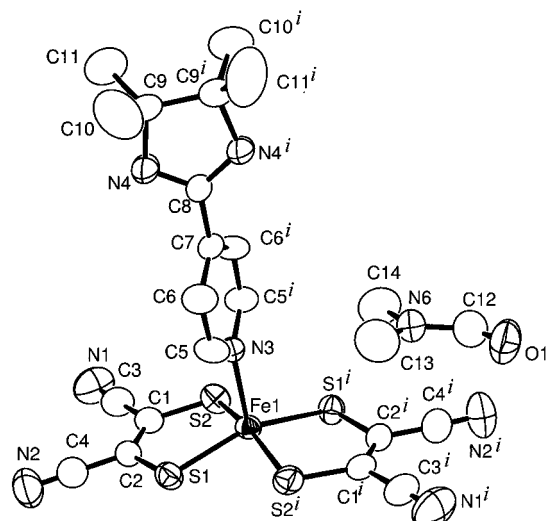
(9) *International Tables for X-ray Crystallography*; Kynoch Press: Birmingham, U.K., 1974; Vol. IV.

(10) Sheldrick G. M. *SHELX 97: Program for the Refinement of Crystal Structures*; University of Göttingen: Germany, 1997.

**Table 2.** Selected Bond Lengths [Å] and Angles [deg]<sup>a</sup>

Fe(1)–N(3)	2.192(3)	Fe(1)–S(2)	2.234(2)
Fe(1)–S(1)	2.235(3)	N(4)–C(8)	1.297(3)
N(4)–C(9)	1.477(4)	C(5)–N(3)	1.324(4)
N(3)–Fe(1)–S(2)	98.14(3)	S(2) <sup>i</sup> –Fe(1)–S(2)	163.73(6)
N(3)–Fe(1)–S(1)	101.56(3)	S(2)–Fe(1)–S(1)	89.42(7)
S(2)–Fe(1)–S(1) <sup>i</sup>	87.33(7)	S(1) <sup>i</sup> –Fe(1)–S(1)	156.88(6)
C(8)–N(4)–C(9)	112.2(3)	C(5)–N(3)–C(5) <sup>i</sup>	117.0(4)
C(5)–N(3)–Fe(1)	121.52(19)		

<sup>a</sup> Symmetry transformation used to generate equivalent atoms: (i)  $-x, y, -z + 1/2$ .

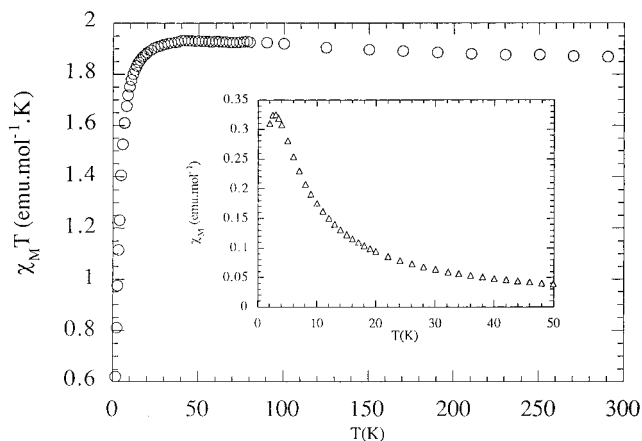
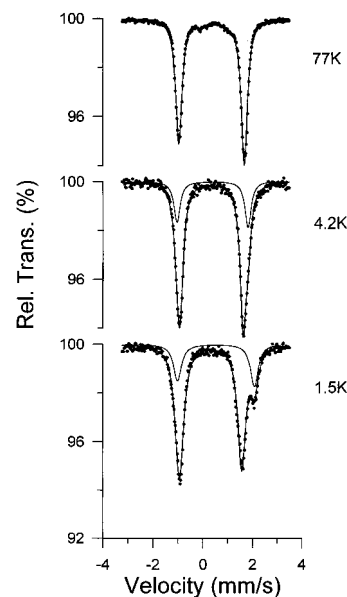
**Figure 1.** ORTEP view of  $\text{Fe}(\text{mnt})_2(\text{idzm}) \cdot 2\text{DMF}$ .

**Magnetic Measurements.** All magnetic studies were carried out on powder samples. Magnetic susceptibility measurements were performed at 0.1 T after zero field cooling, in the temperature range 2–300 K with a SQUID magnetometer “MPMS-5” from Quantum Design Corporation.

**Mössbauer Measurements.** The Mössbauer measurements were obtained on a constant-acceleration spectrometer with a 25 mCi source of  $^{57}\text{Co}$  (in Rh matrix). Isomer shift values are given with respect to metallic iron at room temperature. The absorber was a sample of about 60 mg of microcrystalline powder spread over a 16-mm diameter sample holder made of a pure aluminum foil. Variable temperatures were obtained in a bath cryostat, MD306 Oxford Instruments connected to a temperature controller, ITC4 Oxford Instruments, with Rh–Fe sensor. A least-squares computer program<sup>11</sup> was used to fit the Mössbauer parameters and to determine their standard deviations of statistical origin (given in parentheses).

## Results and Discussion

The molecular structure of the title compound is shown in Figure 1. The molecule is located on a 2-fold axis running through the iron atom and the long axis of the imidazolium unit. As usually observed for other five-coordinated compounds,<sup>6,12</sup> the iron atom adopts square-pyramidal coordination. The imidazolium unit is coordinated to the Fe atom of the  $[\text{Fe}(\text{mnt})_2]^-$  in apical position through the nitrogen atom of the pyridyl ring with the Fe–N3 bond length equal to 2.192(3) Å. The iron atom is displaced out of the four S mean plane toward the center of the pyramid by  $\Delta = 0.382(1)$  Å; this value is close to that observed in the previously reported five coordinated

**Figure 2.** Temperature dependence of  $\chi_M T$  vs  $T$ . Inset: variation of susceptibility  $\chi_M$  vs  $T$ .**Figure 3.** Mössbauer curves at 77, 4.2, and 1.5 K.

molecule with  $\Delta = 0.427(1)$  Å.<sup>6</sup> The Fe–S bond lengths are 2.234(2) and 2.235(3) Å and agree well with those observed in  $[\text{Fe}(\text{mnt})_2(\text{rad})]$ .<sup>6</sup> In the crystal structure the molecules are disposed in columns parallel to the  $b$  axis. In the column the molecules present head-to-tail arrangement but adjacent columns develop in opposite direction. The shortest Fe···Fe separation is 7.304(8) Å. The solvent molecules fill the space fitted by  $\text{Fe}(\text{mnt})_2(\text{idzm})$  molecules. The shortest solvent– $\text{Fe}(\text{mnt})_2(\text{idzm})$  distance is O1–N4 = 2.741(4) Å indicating the existence of hydrogen bonding between the two units. However, the other distances are longer than 3.2 Å, preventing the establishment of bridging contacts between  $\text{Fe}(\text{mnt})_2(\text{idzm})$  units through DMF molecules, thus the molecules can be considered as being magnetically isolated.

The magnetic properties have been investigated in the temperature range 2–300 K. The temperature dependence of both  $\chi_M T$  and the molar susceptibility  $\chi_M$  are represented in Figure 2. The value of  $\chi_M T$  at room temperature is 1.85  $\text{cm}^3 \text{K mol}^{-1}$  which corresponds to the contribution of non interacting quartet spin state arising from Fe(III) atom in intermediate spin ground-state  $S_{\text{Fe}} = 3/2$ .  $\chi_M T$  remains constant down to 40 K and then decreases as the temperature is lowered. At higher temperature range (40–300 K), the magnetic susceptibility closely follows the Curie law ( $\chi_M T = \text{constant}$ ). Below 40 K,

(11) Varret, F. *Proceedings of the International Conference on Applications of the Mössbauer Effect (ICAME'81, Jaipur, India, 1981)*; Indian National Science Academy: New Delhi, 1982; pp 129–140.

(12) For review on 1,2-dithiolato chelates, see: Eisenberg, R. *Prog. Inorg. Chem.* **1970**, *12*, 295–369.

**Table 3.** Fitted Mössbauer Parameters, Isomer Shifts ( $\delta$ ), Quadrupole Splittings ( $\Delta$ ), and Lorentzian Linewidth ( $\Gamma$ , Identical for the Two Components)<sup>a</sup>

<i>T</i> (K)	major doublet		minor doublet		%	$\Gamma$ (mm/s)
	$\delta$ (mm/s)	$\Delta$ (mm/s)	$\delta$ (mm/s)	$\Delta$ (mm/s)		
295	0.262(2)	2.643(4)	—	—	—	0.310(7)
77	0.358(1)	2.640(2)	—	—	—	0.308(3)
4.2	0.354(2)	2.543(5)	0.390(4)	2.86(1)	25	0.304(5)
2.3	0.331(3)	2.534(6)	0.56(1)	3.00(2)	22	0.360(6)
2.1	0.33(1)	2.53(2)	0.57(4)	3.02(7)	21	0.384(8)
1.5	0.330(3)	2.478(5)	0.526(8)	3.10(1)	26	0.384(7)

<sup>a</sup> The standard statistical deviations are given in parentheses. The given percentage is that of the minor doublet.

the decrease of  $\chi_M T$  can be due either to antiferromagnetic interactions or to a spin system modification. The former hypothesis can be ruled out on the basis of the crystal structure data which indicate that the molecules are magnetically rather well isolated. Consequently, intermolecular interactions, if any, should be very weak. However the latter hypothesis warrants thorough investigations since the  $\chi_M$  plot shows a maximum at around 3 K and also, the  $\chi_M T$  value does not tend to zero as  $T$  approaches absolute zero.

Typical Mössbauer spectra are shown in Figure 3; the set of fitted data is listed in Table 3. From room temperature to the liquid nitrogen temperature, the spectra are consistent with the expected spin state  $S = 3/2$ . The slight asymmetry of the doublet is attributed to a texture effect, i.e., a preferred orientation of the crystallites in the sample holder. Also, a small additional doublet was detected, with the larger (relative) proportions at higher temperatures: this is typical for a small amount of iron oxide (nanophased  $\text{Fe}_2\text{O}_3$ ), indicating a slight decomplexation (oxidization) of the sample.

On lowering temperature, mostly below 4 K, the spectra became markedly different, with a second doublet of larger

quadrupole splitting, and higher isomer shift, representing  $\sim 25\%$  of the total area. The clear change in isomer shift gives evidence for a spin change, most probably to the  $S = 1/2$  state; the large quadrupole splitting rules out a  $S = 5/2$  state. The effect was reversible, and on increasing temperature again, the  $S = 3/2$  state was restored. The change appeared to be, so far, rather progressive (spin crossover) than abrupt (spin transition). This is, at our best knowledge, the first example of a  $S = 1/2 \leftrightarrow S = 3/2$  crossover detected by Mössbauer spectroscopy.

### Concluding Remarks

The present spin crossover differs sizably from the well-documented case of the  $\text{Fe}^{\text{II}}$  spin crossover, in the following points; (i) the temperature range where this crossover occurs is extremely low; therefore the observation of the crossover requires the relaxation between the spin states to remain efficient despite of the low thermal activation; a tunneling mechanism is then suggested; (ii) if confirmed by further experiments, the slight variation in the isomer shift of the main doublet, suggests a mixing with the other spin state, consistent with the presence of an efficient tunneling mechanism; (iii) the low-temperature spin crossover might couple to an external magnetic field, or to the magnetization of the system (via the interactions); this makes the situation very attractive at least from the spin-crossover point of view.

**Acknowledgment.** N.M. thanks the Ministerio de Educacion y Cultura (Spain) for a Postdoctoral Fellowship (FIP98).

**Supporting Information Available:** Crystallographic files for crystallographic data, positional parameters, anisotropic thermal parameters, bond lengths and angles, in CIF format, are available free of charge via the Internet at <http://pubs.acs.org>.

IC990299Q